Photooxidation Pathway of Chlorophyll Z in Photosystem II as Studied by Fourier Transform Infrared Spectroscopy†

Yuichi Kitajima and Takumi Noguchi*

Institute of Materials Science, University of Tsukuba, Tsukuba, Ibaraki 305-8573, Japan

Received November 17, 2005; Revised Manuscript Received December 25, 2005

ABSTRACT: The oxidation pathway of chlorophyll Z (Chl_Z) in photosystem II (PSII) at cryogenic temperatures was studied by means of light-induced Fourier transform infrared (FTIR) difference spectroscopy. To examine the involvement of redox-active β-carotene (Car) in the pathway, two Car molecules in Mn-depleted PSII membranes of spinach were selectively bleached by illumination at 250 K in the presence of ferricyanide and silicomolybdate. Successful bleaching of Car was demonstrated by disappearance of the light-induced FTIR signals of Car^+ at 1465, 1440, and 1147 cm^{-1} at 80 K under an oxidative condition. Even in the Car-bleached PSII, the Chl_Z^+/Chl_Z signal at 1713/1687 cm^{-1}, which is attributed to the upshift of the 9-keto C═O band of Chl_Z upon its oxidation, was induced by illumination at 80 K retaining about 80% of the intensity of the control PSII sample. The concomitant appearance of shoulders at 1727/1699 cm^{-1} may indicate that both of the two Chl_Z molecules on the D1 and D2 sides are photooxidized. The multiphasic kinetics of formation of the Chl_Z^+/Chl_Z signal by continuous illumination at 80 K were mostly unchanged by Car depletion, while the formation rates at 210 K were appreciably reduced in Car-bleached PSII. These results indicate that there are electron-transfer pathways from Chl_Z to $P680^+$ that do not involve Car, and they are indeed dominant at 80 K. Although the pathways via Car are mostly blocked at this temperature, the contribution of such pathways to Chl_Z oxidation becomes significant at higher temperatures.

Photosystem II (PSII)[1] is a multimeric protein complex that functions as a light-driven water-quinone oxidoreductase in the photosynthetic electron transport chain. For this function of water oxidation in PSII, the cation radical of the primary donor chlorophyll, $P680^+$, has an extremely high redox potential of 1.1−1.3 V (*1, 2*). To protect the PSII proteins from oxidative damage by this strong oxidant, the secondary electron donation pathway works in PSII when the main pathway from the water oxidizing center is impaired or blocked at cryogenic temperatures (*3*−*7*). This secondary pathway consists of Cyt*b*559, β-carotene (Car), and accessory chlorophyll designated as Chl_Z. They form a cyclic electron-transfer pathway to leak a hole on $P680^+$ to the electron acceptor side. In addition, Chl_Z^+ is proposed to play a role as a quencher of excitation energy under high light condition (*8, 9*).

There are two Chl_Z molecules in PSII, which are symmetrically located in the reaction center (*10*−*13*). The ligands to their central Mg atoms are D1−H118 and D2−H118 (D2−H117 in some organisms) (*14*−*16*), and hence they are designated as Chl_Z(D1) and Chl_Z(D2), respectively. Which Chl_Z is photooxidized is still controversial; in studies using site-directed mutants at D1−H118 and D2−H117, Stewart et al. (*15*) proposed that Chl_Z(D1) is oxidized in the cyanobacterium *Synechocystis* 6803, while Wang et al. (*16*) proposed Chl_Z(D2) as an oxidized chlorophyll in *Chlamydomonas reinhardtii*. In addition, Tracewell et al. (*17*) analyzed the near-infrared absorption bands of Chl_Z^+ and concluded that both Chl_Z(D1) and Chl_Z(D2) are photooxidized in spinach.

There are also two redox-active Car molecules in the PSII reaction center (*4*−*7, 18*−*29*). The positions of these Car molecules, however, have not yet been definitely determined by X-ray crystallography (*10*−*13, 30*). Kamiya and Shen (*12, 30*) showed that both Car molecules are attached to the D2 subunit in their X-ray crystal structure of the PSII core complex from *Thermosynechococcus vulcanus* at 3.7 Å resolution. On the other hand, in the crystal structures of *Thermosynechococcus elongatus* by Ferreira et al. (3.5 Å resolution) (*10*) and Biesiadka et al. (3.2 Å resolution) (*11*), only one Car was resolved on the D2 subunit. Very recently, Loll et al. (*13*) reported the 3.0 Å resolution structure of *T. elongatus*, in which another Car is attached to the D1 subunit near Chl_Z(D1). Thus, all of these structures [for *T. vulcanus*, the revised one (*30*)] showed a common all-trans Car near Chl_Z(D2), whereas the position of the other Car is still controversial. Only a single Cyt*b*559 on the D2 side was found in the X-ray structures of PSII in both *T. vulcanus* and *T. elongatus* (*10*−*13*).

† This study was supported by a Grant-in-Aid for Scientific Research (17GS0314) from the Ministry of Education, Culture, Sports, Science and Technology of Japan, and by Special Research Project "Nano-Science" at University of Tsukuba.

* To whom correspondence should be addressed. Phone: +81-29-853-5126. Fax: +81-29-855-7440. E-mail: tnoguchi@ims.tsukuba.ac.jp.

[1] Abbreviations: Car, the redox-active β-carotene in photosystem II.; Chl_Z, the redox-active accessory chlorophyll in photosytem II; Cyt*b*559, cytochrome *b*559; FTIR, Fourier transform infrared; Mes, 2-(*N*-morpholino)ethanesulfonic acid; PSII, photosystem II.; P680, the primary electron donor chlorophyll of photosystem II; SiMo, silicomolybdate.

10.1021/bi052346y CCC: $33.50
Published on Web 01/24/2006

The secondary electron-transfer pathway to $P680^+$ involving Car, Chl_Z, and Cyt*b*559 has been extensively argued (*3*−*7*, *17*, *23*−*25*, *31*−*35*). There is general agreement that Cyt*b*559 is the last oxidized component (*3*, *23*−*25*, *32*), which accepts an electron from Q_B^- (*36*). Most works also agree that Car is an initial electron donor to $P680^+$ and mediates the oxidation of Cyt*b*559 (*4*−*7*, *23*, *25*). Very recent work by Bautista et al. (*37*) using the PSII complexes of the *Synechocystis* mutants which contain carotenoids with shorter π-conjugation than β-carotene showed that the redox potential of Car^+ is an important factor in Car oxidation.

It is generally thought that Chl_Z is oxidized via Car (*4*, *6*, *7*, *23*, *25*, *26*, *38*, *39*), based on the observations that Car^+ is trapped to a larger extent than Chl_Z at lower temperatures (*21*, *23*, *26*) and the trapped Car^+ is mostly replaced with Chl_Z^+ by warming up the sample (*23*, *25*, *38*, *39*). This electron-transfer pathway ($P680^+ \leftarrow Car \leftarrow Chl_Z$) is consistent with the relative positions of these pigments on the D2 side in the X-ray structure of all three groups (*10*−*13*, *30*) and on the D1 side in the new structure of *T. elongatus* by Loll et al. (*13*); the Car molecules are positioned between P680 and Chl_Z. This pathway, however, was inconvenient for the oxidation of Chl_Z(D1) in the context of the X-ray structure of *T. vulcanus* (*30*) and the previous structures of *T. elongatus* (*10*, *11*), in which no Car was found on the D1 side. To circumvent this difficulty, an electron-transfer route from Chl_Z(D1) to Car^+ via several Chl molecules in the CP43 protein was proposed (*34*). The presence of this route was further supported by theoretical calculations of the redox potentials of the Car and Chl molecules in the PSII core complex (*35*).

In this study, light-induced FTIR difference spectroscopy was used to investigate the oxidation pathway of Chl_Z, especially focusing on the involvement of Car in the pathway. This spectroscopic method has been used to study the structures and reactions of various redox cofactors in PSII (*40*). Characteristic FTIR signals upon photooxidation of Car (*21*) and Chl_Z (*41*) have been observed, and thus they can be used as good markers to monitor the photooxidation of Car and Chl_Z under various conditions. For the above purpose, we have selectively bleached the redox-active Car molecules in PSII membranes of spinach by illumination at 250 K. Using this Car-bleached PSII, photooxidation of Chl_Z was examined at cryogenic temperatures. We have found that the Chl_Z molecules were oxidized even after Car depletion, suggesting the presence of the oxidation pathway of Chl_Z that does not involve Car. It was also shown that this pathway is dominant at 80 K, while the contribution of the pathway via Car becomes significant by increasing temperature.

MATERIALS AND METHODS

PSII membranes were prepared from spinach following the method by Ono and Inoue (*42*) and suspended in a Mes buffer (40 mM Mes−NaOH, 400 mM sucrose and 20 mM NaCl, pH 6.5). Mn depletion of the PSII membranes was performed with NH_2OH treatment (10 mM) followed by several washes with the Mes buffer.

The "250 K illumination treatment" on the PSII membranes to bleach redox-active Car molecules was performed as follows. Suspension of the Mn-depleted PSII membranes (0.25 mg Chl/mL; 250 μL) in the Mes buffer including 20 mM potassium ferricyanide, 0.3 mM SiMo, and 50% (v/v) glycerol was placed in a cuvette with an optical path length of 4 mm and a width of 8 mm. The sample in a cryostat (Oxford DN1704), in which the temperature was adjusted to 250 K using a controller (Oxford ITC-4), was illuminated with white light from a tungsten lamp (Cabin ME-650) with an intensity of $\sim$1.0 W/cm^2 at the sample surface. Several samples were collected and washed with the Mes buffer.

FTIR spectra were recorded on a Bruker IFS-66/S spectrophotometer equipped with an MCT detector (InfraRed D316/8) at a resolution of 4 cm^{-1}. For preparation of a sample for FTIR measurements, a suspension of the PSII membranes (0.5 mg Chl/mL) in the Mes buffer (pH 6.5) including 40 mM potassium ferricyanide and 0.6 mM SiMo as electron acceptors was centrifuged (150000*g*) for 30 min. The resultant pellets were placed between a pair of BaF_2 plates (13 mm in diameter). The sample temperature was controlled in the cryostat (Oxford DN1704). Light-induced difference spectra were obtained by measurements of single-beam spectra (scanning mode: double-sided fast return) before and after illumination by continuous white light ($\sim$35 mW/cm^2 at the sample surface) from a halogen lamp (Hoya-shott HL150). When intensities of the difference spectra recorded using different samples were compared with each other, spectra were normalized on the basis of the amide II intensity ($\sim$1554 cm^{-1}) in the absorption spectra of the PSII samples.

RESULTS

To selectively bleach the redox-active Car molecules in PSII, Mn-deleted PSII membranes of spinach were illuminated with strong white light at 250 K in the presence of 20 mM ferricyanide and 0.3 mM SiMo ("250 K illumination treatment").

Figure 1 shows the effects of this treatment on the Car^+-Chl_Z^+/CarChl_Z FTIR difference spectrum recorded at 80 K in the presence of 40 mM ferricyanide and 0.6 mM SiMo as electron acceptors. Note that under this oxidative condition, Cyt*b*559 is preoxidized and hence does not show bands in the FTIR difference spectra. The typical Q_A^- signal at 1478 cm^{-1} due to the CO stretching vibration of a semiquinone anion (*43*) was not observed in the spectra in Figure 1, indicating that Q_A^- was not accumulated by illumination; SiMo can abstract an electron from Q_A and/or pheophytin even at 80 K. Thus, under this condition, more than one oxidizing equivalent can be accumulated on the donor side of PSII.

The spectrum of the control Mn-depleted PSII sample (Figure 1a) showed strong positive peaks at 1465, 1440, and 1147 cm^{-1}, which have been assigned to the C═C (1465 and 1440 cm^{-1}) and C−C (1147 cm^{-1}) stretching vibrations of photoinduced Car^+ in PSII (*21*). The split peaks at 1465 and 1440 cm^{-1} most probably arise from the two distinct Car molecules oxidized by $P680^+$, because the predominant peak at 1440 cm^{-1} was observed in the previous FTIR study using the D1−D2−Cyt*b*559 complex in the presence of ferricyanide (*44*). In the latter study, one of the two Car molecules (Car_{507}) was asserted to be preferentially oxidized based on the absorption changes in the visible region (*44*). This preference of Car oxidation seems to depend on

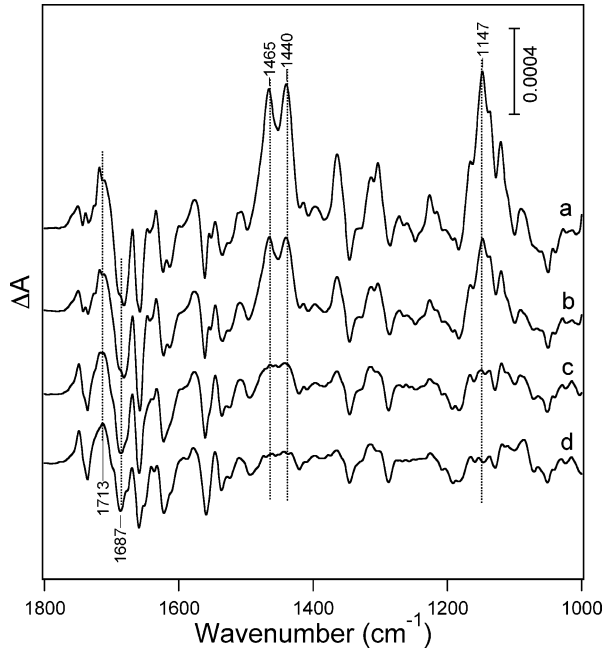

FIGURE 1: Light-induced FTIR difference spectra of $Chl_Z^+Car^+$/Chl_ZCar recorded at 80 K using Mn-depleted PSII membranes subjected to "250 K illumination treatment" for 0 (a), 3 (b), 5 (c), and 10 (d) min. In the 250 K illumination treatment, Mn-depleted PSII membranes in a Mes buffer (pH 6.5) in the presence of 20 mM potassium ferricyanide, 0.3 mM SiMo, and 50% (v/v) glycerol were illuminated by strong continuous light (~1.0 W/cm^2) for a given period at 250 K. The samples were then washed with the Mes buffer. In FTIR measurements at 80 K, PSII samples in the presence of 40 mM potassium ferricyanide and 0.6 mM SiMo were illuminated with white light (~35 mW/cm^2) for 10 s, and FTIR difference spectra as after-minus-before illumination (150-s accumulation for each single-beam spectrum) were recorded. The measurement was repeated after dark relaxation at 285 K, and three spectra were averaged for the final data.

conditions and samples; Telfer et al. (*28*) observed photooxidation of two Car molecules to the same extent in the presence of SiMo. The different peak frequencies at 1465 and 1440 cm^{-1} may indicate that there is some structural difference between the two Car^+ molecules, although further investigation is necessary to definitely identify the origin of the split peaks. In addition to the strong Car^+ bands, a signal typical of the Chl_Z^+/Chl_Z difference (*41*) was also observed at ~1713/1687 cm^{-1} overlapping with neighboring features at 1718 and 1682 cm^{-1} due to Car^+/Car. This differential signal at 1713/1687 cm^{-1} arises from the 9-keto C═O stretching vibrations of Chl_Z^+/Chl_Z (*41*).

In the course of the 250 K illumination treatment, the Car^+ signals at 1465, 1440, and 1147 cm^{-1} gradually decreased, whereas the Chl^+/Chl signal remained in the spectra (Figure 1). The intensities of the Car^+ (1465, 1440, and 1147 cm^{-1}) and Chl_Z^+/Chl_Z (1713/1687 cm^{-1}) signals were plotted against the duration of 250 K illumination treatment in Figure 2. After the treatment for 10 min, all of the three Car^+ signals almost disappeared, while about 80% of the Chl_Z^+/Chl_Z signal remained. This experiment demonstrated that the redox-active Car was selectively bleached by this treatment. The observation that both peaks at 1465 and 1440 cm^{-1} diminished in a similar manner may indicate that the two Car molecules are bleached at the same rate. It is noteworthy that Car bleaching was accelerated in a solution sample rather than in a pellet form (in an FTIR cell), suggesting that

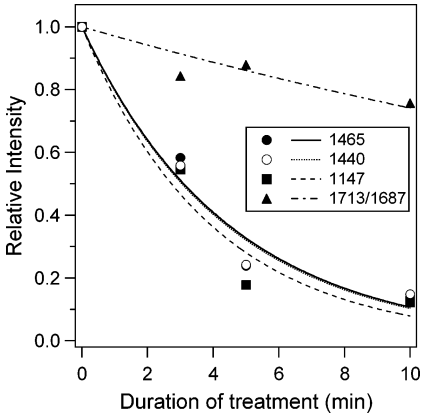

FIGURE 2: Effect of 250 K illumination treatment on the intensities of the FTIR signals of Car^+ and Chl_Z^+ at 80 K. Light-induced FTIR difference spectra were recorded at 80 K in the presence of ferricyanide and SiMo (Figure 1). Relative intensities of the peaks at 1465 (closed circle), 1440 (open circle), 1147 (closed square) cm^{-1} as Car^+ signals and of the differential band at 1713/1687 cm^{-1} (closed triangle) as a Chl_Z^+/Chl_Z signal were plotted as a function of the duration of 250 K illumination treatment.

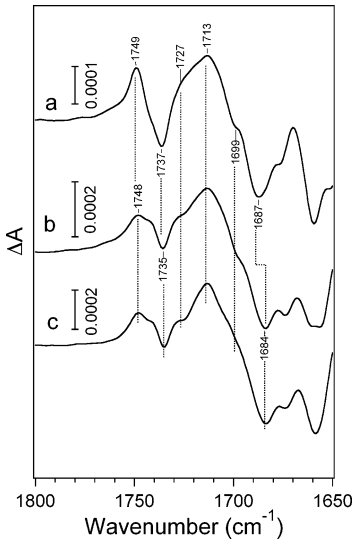

FIGURE 3: Keto and ester C═O stretching region of the Chl_Z^+/Chl_Z FTIR spectra of Car-bleached PSII (a, b) in comparison with the Chl_Z^+/Chl_Z spectrum of control Mn-depleted PSII (c). Light-induced FTIR difference spectra were recorded at 80 (a) and 210 (b, c) K. Car bleaching of Mn-depleted PSII membranes was performed by 250 K illumination treatment for 10 min. Single-beam FTIR spectra (150-s accumulation) were recorded before and after 10-s illumination, and difference spectra were calculated. For the spectrum at 80 K (a), the results of three measurements were averaged.

destruction of Car requires an aerobic condition. Also, the Car bleaching may take place via Car^+, because when the photoreaction of the PSII sample under a similar condition (but in a pellet form, i.e., with less oxygen) was monitored with visible and near-infrared spectra at 250 K, a broad positive signal at 900−1000 nm due to Car^+ was observed concomitant with negative peaks by bleaching of neutral Car at 506, 489, 473, and 441 nm (data not shown). Hereafter, the Mn-depleted PSII sample in which Car is almost fully bleached by the 250 K illumination treatment for 10 min will be denoted as Car-bleached PSII.

Figure 3 shows the keto and ester C═O stretching region of the light-induced Chl_Z^+/Chl_Z FTIR difference spectra of the Car-bleached PSII membranes recorded at 80 (a) and

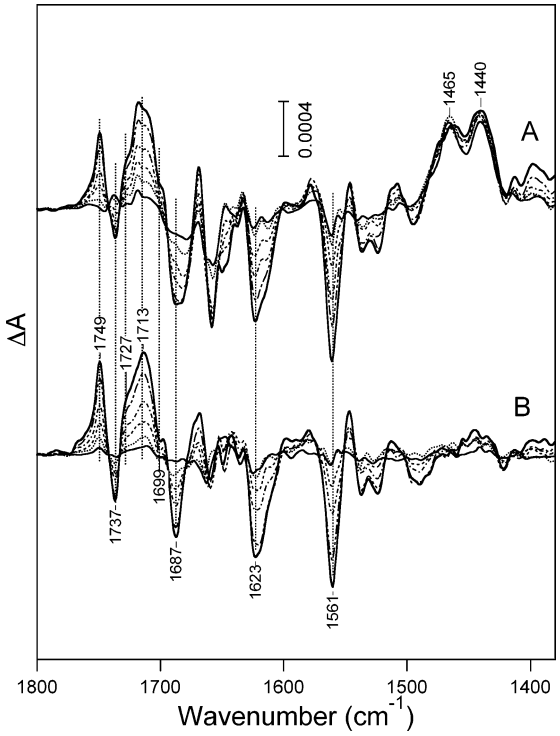

FIGURE 4: $Chl_Z^+Car^+/Chl_ZCar$ FTIR difference spectra of control Mn-depleted PSII (A) and Chl_Z^+/Chl_Z spectra of Car-bleached PSII (B) recorded at 80 K upon illumination for 1 (thin —), 5 (•••), 20 (- - -), 60 (-•-•), 300 (-•••-••), and 900 (bold —) s. The sample was illuminated with white light (~35 mW/cm^2) in the presence of 40 mM potassium ferricyanide and 0.6 mM SiMo, and single-beam FITR spectra were recorded for 15 s before and after a certain period of illumination to calculate light-induced difference spectra. All the spectra in panel A or B were measured using a single sample in the course of illumination. Because the shutter in the light path was closed during spectral scans, the illumination time represents a net period of illumination.

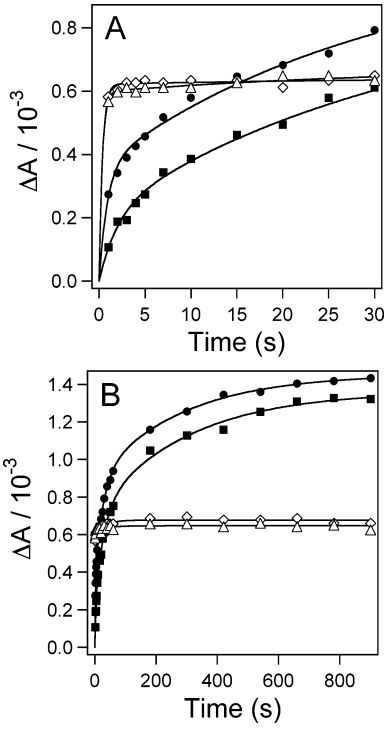

FIGURE 5: Time course of the formation of the Car^+ and Chl_Z^+ signals in the FTIR difference spectra upon illumination at 80 K in the presence of ferricyanide and SiMo. Panels A and B show the time regimes of 0−30 and 0−900 s, respectively. The intensities of the Car^+ peaks at 1465 (open triangle) and 1440 (open diamond) cm^{-1} of control PSII and the intensity of the Chl_Z^+/Chl_Z signal at 1713/1687 cm^{-1} of control (closed circle) and Car-bleached (closed square) PSII samples (Figure 4) were plotted as a function of illumination time. The solid curves are the results of multiexponential fitting.

210 (b) K and that of control Mn-depleted PSII membranes recorded at 210 K (c). Note that Car^+ is not accumulated by illumination at 210 K in the PSII membranes of spinach, and hence a pure Chl_Z^+/Chl_Z spectrum can be obtained in the control sample at this temperature (*41*). The three spectra exhibited common prominent features. In the 9-keto C═O region, the large positive peak at 1713 cm^{-1} due to Chl_Z^+ and the corresponding negative peak at 1687−1684 cm^{-1} due to neutral Chl_Z (*41*) were observed. In addition, the positive shoulder at 1727 cm^{-1} seems to correspond to the negative shoulder at 1699 cm^{-1}, although the latter was not very clear in the spectrum of the control PSII sample (Figure 3c). The positive/negative peaks at 1749−1748/1737−1735 cm^{-1} in the ester C═O region most probably arise from the 10a-ester C═O vibrations of Chl_Z^+/Chl_Z (*41*). Thus, the Chl_Z^+/Chl_Z spectra in the Car-bleached PSII were basically identical to the spectrum of the control PSII sample, except that the bands were slightly broader in Car-bleached PSII even when compared at the same temperature of 210 K (Figure 3b,c).

Figure 4 shows the development of the FTIR signals during illumination at 80 K for the control (A) and Car-bleached (B) PSII samples. The samples include 40 mM ferricyanide and 0.6 mM SiMo as electron acceptors, and FTIR spectra were recorded in the course of white light illumination (~35 mW/cm^2 at sample). Although a shutter in a light path was closed during spectral scans to avoid contamination by P680 signals, this dark period does not affect the time course of cation formation because the relaxation times of Car^+ and Chl_Z^+ under this condition are very slow (see below). In the control Mn-depleted PSII (Figure 4A), the Car^+ signals at 1465 and 1440 cm^{-1} fully appeared by 1-s illumination and the intensities did not change by further illumination. In the Car-depleted PSII (Figure 4B), on the other hand, the Car^+ signals did not appear even after long illumination (900 s), confirming that the redox-active Car is indeed bleached and that the disappearance of the Car^+ signals observed in Figures 1 and 2 is not ascribed to a reduced rate of Car^+ formation. In sharp contrast to the formation kinetics of the Car^+ signals, the Chl_Z^+/Chl_Z signals at 1749, 1737, 1727, 1713, 1687, 1623, and 1561 cm^{-1} gradually increased by prolonged illumination in both control (Figure 4A) and Car-bleached (Figure 4B) PSII. Note that our previous study using PSII membranes of spinach showed that a slight increase in local sample temperature by long illumination induced a prominent negative peak at 1559 cm^{-1} in FTIR difference spectra without large structures around 1700 cm^{-1} (*45*). Thus, the negative feature at 1561 cm^{-1} might include some contribution of thermal effects by illumination, but it will be safe to estimate the Chl_Z^+ formation using the keto C═O signal at 1713/1687 cm^{-1}.

The time courses of the intensities of the Car^+ and Chl_Z^+ signals are shown in Figure 5 (A, 0−30 s; B, 0−900 s). In control PSII membranes, both Car^+ signals at 1465 (open triangle) and 1440 (open diamond) cm^{-1} are immediately

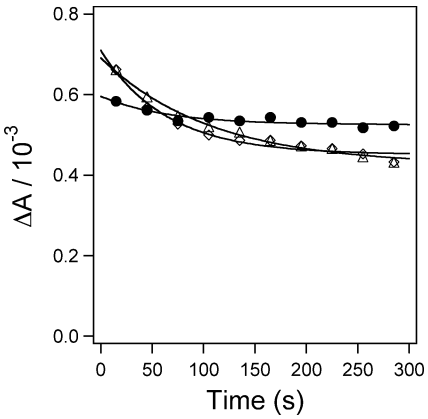

FIGURE 6: Relaxation of the Car^+ signals at 1465 (open triangle) and 1440 (open diamond) cm^{-1} and of the Chl_Z^+/Chl_Z signal at 1713/1687 cm^{-1} (closed circle) after illumination of Mn-depleted PSII membranes for 10 s at 80 K.

formed and saturated in a few seconds, while the Chl_Z^+/Chl_Z signal at 1713/1687 cm^{-1} (closed circle) developed rather slowly and needed more than 900 s to reach the maximum. The formation kinetics of this Chl_Z signal can be fitted by three exponential functions with time constants of 0.9 ± 0.1 (25%), 26 ± 3 (36%), and 283 ± 30 (39%) s. The rate of the fastest phase could be inaccurate because of the partial overlap of the Chl_Z^+/Chl_Z bands with the Car^+/Car signals at 1718 and 1682 cm^{-1} (Figure 4A). In Car-bleached PSII, the similar formation kinetics of Chl_Z^+/Chl_Z signal (closed square) were observed with time constants of 1.9 ± 0.5 (15%), 28 ± 4 (37%), and 301 ± 38 (48%) s. Note that the slightly lower saturation intensity of this signal at 900 s compared with that of control PSII is ascribed to the partial inactivation of Chl_Z by 250 K illumination treatment.

Figure 6 shows the relaxation of the Car^+ and Chl_Z^+ signals of the control PSII sample induced by illumination for 10 s at 80 K. By this illumination, Car^+ is fully accumulated, whereas Chl_Z^+ is formed only in ~40% of the maximum level (Figure 5). The Car^+ signals at 1465 and 1440 cm^{-1} seemed to show a multiphasic decay in agreement with the previous observation (*17*), and the fast phase (~30%) relaxed in ~150 s. The Chl_Z^+/Chl_Z signal at 1713/1687 cm^{-1} was very stable up to 300 s, and the increase of the Chl_Z^+ signal at the expense of Car^+ was not observed.

The time evolution of the FTIR signals by continuous illumination was also examined at 210 K. The spectra are shown in Figure 7 (A, control PSII; B, Car-bleached PSII), and the time course of the Chl_Z^+/Chl_Z signal at 1713/1684 cm^{-1} is plotted in Figure 8 (A, 0−60 s; B, 0−900 s). The signal formation in control PSII (Figure 8, closed circle) can be fitted by three exponentials with time constants of 0.6 ± 0.1 (41%), 11 ± 1 (37%), and 249 ± 63 (22%) s, and that in Car-bleached PSII (Figure 8, closed square) with time constants of 1.3 ± 0.3 (23%), 33 ± 9 (33%), and 290 ± 69 (44%) s. All the phases were clearly slowed in Car-bleached PSII and the relative amount of the slowest phase was doubled at the expense of the fastest phase. Thus, the Chl_Z^+ formation kinetics was affected by Car depletion more significantly at 210 K than at 80 K.

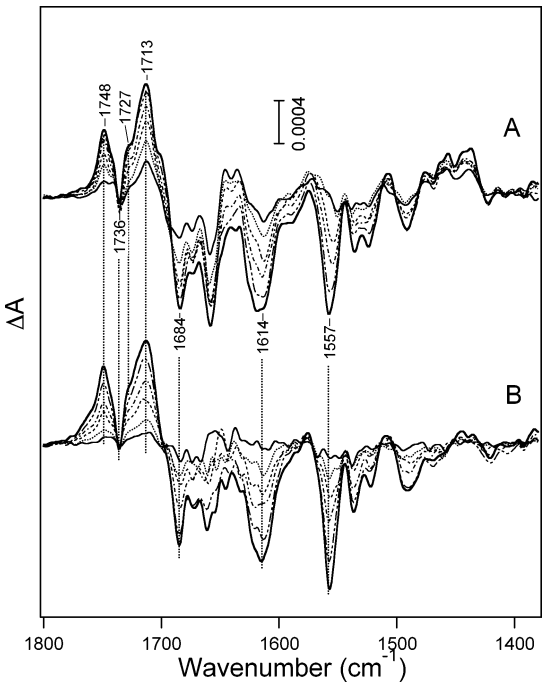

FIGURE 7: Chl_Z^+/Chl_Z FTIR difference spectra of control (A) and Car-bleached (B) PSII recorded at 210 K upon illumination for 1 (thin —), 5 (•••), 20 (- - -), 60 (-•-•), 300 (-••-••), and 900 (bold —) s. The measurement conditions were the same as those for Figure 4 except for the temperature of 210 K and scanning time of 10 s.

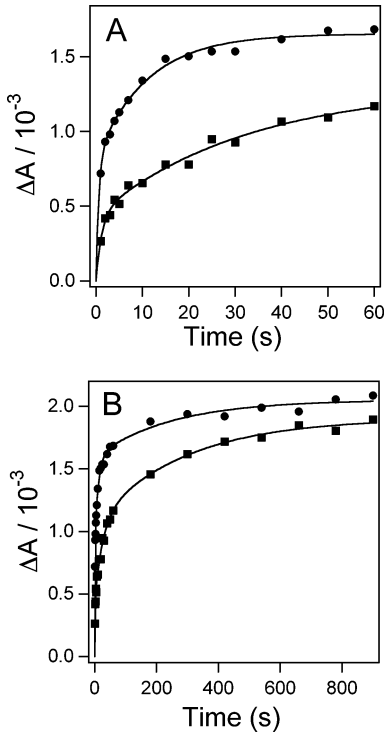

FIGURE 8: Time course of the formation of the Chl_Z^+ signals in the FTIR difference spectra upon illumination at 210 K in the presence of ferricyanide and SiMo. Panels A and B show the time regimes of 0−60 and 0−900 s, respectively. The intensities of the Chl_Z^+/Chl_Z signal at 1713/1684 cm^{-1} of the control (closed circle) and Car-bleached (closed square) PSII samples (Figure 7) were plotted as a function of illumination time. The solid curves are the results of multiexponential fitting.

DISCUSSION

In the present study, two redox-active Car molecules in Mn-depleted PSII membranes were selectively bleached by strong-light illumination at 250 K under oxidizing condition, as demonstrated by disappearance of the characteristic FTIR signals of Car^+ at 1465, 1440, and 1147 cm^{-1} at 80 K

(Figures 1 and 2). Similar Car bleaching via its cation has been reported in the PSII reaction center complex at 10 °C (*19*) and 250 K (*44*). Even in the PSII membranes almost fully depleted of Car, ~80% of Chl_Z was intact and capable of photooxidation (Figure 2). Because this Car bleaching seemed to require oxygen under our condition (but see ref 19), it is presumed that Car^+ reacts with oxygen to disrupt C=C bonds or to form peroxide or epoxy compounds (*46*−*48*). HPLC analysis of this Car-depleted PSII preparation did not detect a meaningful amount of newly formed carotenoid at the expense of β-carotene (Takaichi, unpublished data). Thus, redox-active Car in PSII may be destroyed and released from the binding pocket; at least, a carotenoid with more than three conjugated C=C bonds may not be left in the pocket.

The Chl_Z^+/Chl_Z spectrum of Car-bleached PSII recorded at 80 K showed a prominent differential signal at 1713(+)/1687(−) cm^{-1} with a pair of shoulders at 1727(+)/1699(−) cm^{-1} in the region of the 9-keto C=O stretch, and a differential signal at 1749(+)/1737(−) cm^{-1} in the ester C=O region (Figure 3a). The corresponding bands were observed at 1713/1684, 1727/1699, and 1748/1735 cm^{-1} at 210 K (Figure 3b), and these features were basically identical to those of control PSII membranes (Figure 3c). Thus, Car depletion virtually did not affect the structure and interaction of Chl_Z, suggesting that there is no strong molecular interaction between Car and Chl_Z. Slight broadening of bands in Car-bleached PSII (Figure 3b) in comparison with the control sample (Figure 3c) could be ascribed to a subtle structural perturbation of the reaction center proteins by Car depletion. The upshifts of the C=O bands upon Chl_Z^+ formation, i.e., 26−29 and 28 cm^{-1} for the 1713/1684−1687 and 1727/1699 cm^{-1} bands of the 9-keto C=O, and 12−13 cm^{-1} for the 1748−1749/1735−1737 cm^{-1} bands of the ester C=O, are in good agreement with the upshifts by 25 and 13 cm^{-1} of the 9-keto and 10a-ester C=O bands of free Chl*a* in THF upon cation formation (*49*). The presence of two sets of keto C=O bands in Chl_Z^+/Chl_Z spectra is consistent with the view by Tracewell et al. (*17*) that both Chl_Z(D1) and Chl_Z(D2) are photooxidized in spinach. It is presumed that the 9-keto C=O group of Chl_Z with the 1713/1684−1687 cm^{-1} bands is weakly H-bonded or located in a polar environment, while that of the other Chl_Z with the 1727/1699 cm^{-1} bands is located in a rather hydrophobic environment. The assignment of the two keto C=O signals to individual Chl_Z molecules on the D1 and D2 sides and how the apparent intensity difference between the 1713 and 1727 cm^{-1} bands reflects the difference in population of the two Chl_Z cations are unknown at present. Also, the possibility that the signals of Chl molecules in CP43 or CP47 in redox equilibrium with Chl_Z^+ are included in the observed spectra cannot be excluded. Further comparative studies using cyanobacteria and *Chlamydomonas* in combination with site-directed mutagenesis will be necessary to answer these questions.

When the control PSII sample is illuminated by continuous light at 80 K in the presence of ferricyanide and SiMo, the Car^+ signals at 1465 and 1440 cm^{-1} were immediately formed within 1 s, whereas the Chl_Z^+ signal at 1713/1687 cm^{-1} developed more slowly with three phases with time constants of ~1, ~26, and ~280 s (Figures 4 and 5). The formation kinetics of Chl_Z^+ was basically unchanged in Car-bleached PSII, except that the time constant of the fastest phase seems to become slightly slower and the relative amount of the slowest phase increased by ~9% at the expense of the fastest phase. Multiphasic kinetics of Chl_Z^+ formation may be ascribed to the heterogeneity of PSII proteins, consistent with the multiphasic decay of Car^+ previously reported (*17*) and also observed in this study (Figure 6). The above observation of the similar kinetics of Chl_Z^+ formation between the control and Car-bleached PSII samples indicates that the major pathway of Chl_Z oxidation at 80 K does not involve Car. Since the positive shoulder at 1727 cm^{-1} basically followed the behavior of the 1713 cm^{-1} band (Figure 4), this conclusion may hold for both Chl_Z(D1) and Chl_Z(D2). The electron transfer from Chl_Z to Car^+ may be mostly blocked at this temperature of 80 K. The absence of additional formation of Chl_Z^+ in the dark after illumination for 10 s (Figure 6), by which Car^+ was fully accumulated but less than half of Chl_Z^+ was formed in the PSII sample, supports this idea.

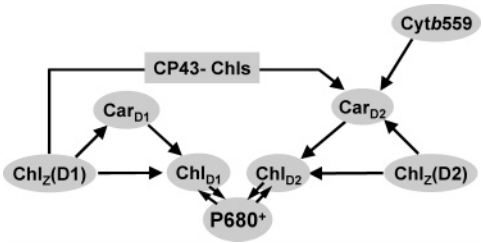

FIGURE 9: Proposed electron-transfer pathways in photooxidation of the Chl_Z molecules. The pathways from Chl_Z(D1) and Chl_Z(D2) to $P680^+$ (probably via Chl_{D1}, Chl_{D2}) without involving Car are dominant at 80 K, while the pathways via Car become significant at 210 K. One Car molecule (Car_{D2}) is located near Chl_Z(D2), and another Car has been resolved on the D2 side in the X-ray structure (3.7 Å) of *T. vulcanus* (*30*) and on the D1 side in the structure (3.0 Å) of *T. elongatus* (*13*). Here, the latter structure with high resolution was adopted (Car_{D1}). The pathway from Chl_Z(D1) to Car_{D2} via several Chl molecules in CP43 has been proposed (*34*, *35*).

Under illumination at 210 K, on the other hand, the time constants of all three phases of Chl_Z^+ formation were slowed down by Car depletion from <1, ~10, and ~250 s to ~1, ~30, and ~300 s, respectively, and the relative amount of the fastest phase in control PSII (41%) was almost halved in Car-bleached PSII (23%) to be replaced by the slowest phase (Figure 8). Thus, the contribution of the pathway via Car to the mechanism of Chl_Z oxidation is more significant at 210 K. In other words, electron transfer from Chl_Z to Car^+ is allowed at relatively high temperatures.

The electron-transfer pathways from Chl_Z to $P680^+$ proposed in this study are summarized in Figure 9, taking into account the pigment positions in the X-ray structures of PSII (*10*−*13*, *30*), especially the recent structure by Loll et al. (*13*) as to the Car positions, and the previously proposed pathways involving Car, Chl_Z, and Cyt*b*559 (*4*,*5*, *7*, *17*, *23*, *25*, *32*, *34*, *35*). There are electron-transfer pathways from Chl_Z(D1) and Chl_Z(D2) to $P680^+$ that do not involve Car, and indeed these pathways are dominant at 80 K. The accessory Chl molecules, Chl_{D1} and Chl_{D2}, neighboring P680 may be involved in the electron transfer as transient intermediates. The kinetic rates of these Chl_Z-to-$P680^+$ pathways, however, are much slower than the rate of the electron transfer from Car to $P680^+$, being consistent with the longer distances between Chl_{D1}/Chl_{D2} and Chl_Z(D1)/Chl_Z-

(D2) than those between Chl_{D1}/Chl_{D2} and Car_{D1}/Car_{D2} (*10*−*13*, *30*). At 80 K, electron transfer from Chl_Z to Car^+ is blocked, but at a higher temperature of 210 K, this pathway is allowed and makes appreciable contribution to Chl_Z oxidation. The plausible explanation for this difference between 80 and 210 K is that the relative levels of the redox potentials of Car and Chl_Z change depending on temperature and the potential of Car is higher than that of Chl_Z at 210 K but becomes lower by decreasing the temperature to 80 K. Electron transfer from Chl_Z(D1) to Car_{D2}^+ via several Chl molecules in CP43 has been proposed and supported by theoretical calculations (*34*, *35*).

The above view is consistent with the observations reported so far about the Car and Chl_Z oxidation in PSII. At very low temperatures (≤20 K), Car^+ is predominantly formed by a single-electron reaction in which Q_A^- is accumulated on the acceptor side (*23*, *25*, *26*). Under this condition, the quantity ratio of accumulated Chl_Z^+ to Car^+ is determined by the kinetic rates of the electron transfer from Chl_Z to $P680^+$ relative to that from Car to $P680^+$. Because the electron-transfer rate from Car to $P680^+$ is much faster than that from Chl_Z at low temperatures (Figure 5), Car^+ should be largely accumulated. Very recently, Bautista et al. (*37*) observed that the Chl_Z^+/Car^+ ratio photoinduced at 20 K is higher in the mutant in which β-carotene is replaced by a carotenoid with a shorter conjugated chain. Because this shorter Car has a higher redox potential than β-carotene (*37*), the rate of Car oxidation by $P680^+$ should be slower in the mutant, naturally resulting in the increased ratio of Chl_Z^+ in the above view. Furthermore, it has been observed that Car^+ trapped at low temperatures was replaced with Chl_Z^+ by warming up the PSII sample to 120 K (*23*, *25*, *38*, *39*). This observation is readily explained by the capability of the electron transfer from Chl_Z to Car^+ at higher temperatures.

ACKNOWLEDGMENT

The authors thank Professor Shinichi Takaichi for HPLC analyses of carotenoids in PSII preparations.

REFERENCES

1. Klimov, V. V., Allakhverdiev, S. I., Demeter, S., and Krasnovskii, A. A. (1979) Photoreduction of pheophytin in the photosystem 2 of chloroplasts with respect to the redox potential of the medium, *Dokl. Akad. Nauk* SSSR *249*, 227−230.
2. Rappaport, F., Guergova-Kuras, M., Nixon, P. J., Diner, B. A., and Lavergne, J. (2002) Kinetics and pathways of charge recombination in photosystem II, *Biochemistry 41*, 8518−8527.
3. Stewart, D. H., and Brudvig G. W. (1998) Cytochrome b_{559} of photosystem II. *Biochim. Biophys. Acta 1367*, 63−87.
4. Tracewell, C. A., Vrettos, J. S., Bautista, J. A., Frank, H. A., and Brudvig, G. W. (2001) Carotenoid photooxidation in photosystem II, *Arch. Biochem. Biophys. 385*, 61−69.
5. Telfer, A. (2002) What is β-carotene doing in the photosystem II reaction centre?, *Philos. Trans. R. Soc. London, B 357*, 1431−1439.
6. Frank, H. A., and Brudvig, G. W. (2004) Redox functions of carotenoids in photosynthesis, *Biochemistry 43*, 8607−8615.
7. Faller, P., Fufezan, C., and Rutherford, A. W. (2005) Side-path electron donors: Cytchrome b_{559}, chlorophyll Z and β-carotene, in *Photosystem II: The Light-Driven Water: Plastoquinone Oxidoreductase* (Wydrzynski, T., and Satoh, K., Eds.) pp 347−365, Springer, Dordrecht, The Netherlands.
8. Schweitzer, R. H., and Brudvig, G. W. (1997) Fluorescence quenching by chlorophyll cations in photosystem II, *Biochemistry 36*, 11351−11359.
9. Schweitzer, R. H., Melkozernov, A. N., Blankenship, R. E., and Brudvig, G. W. (1998) Time-resolved fluorescence measurements of photosystem II: The effect of quenching by oxidized chlorophyll Z, *J. Phys. Chem. B 102*, 8320−8326.
10. Ferreira, K. N., Iverson, T. M., Maghlaoui, K., Barber, J., and Iwata, S. (2004) Architecture of the photosynthetic oxygen-evolving center, *Science 19*, 1831−1838.
11. Biesiadka, J., Loll, B., Kern, J., Irrgang, K. D., and Zouni, A. (2004) Crystal structure of cyanobacterial photosystem II at 3.2 Å resolution: a closer look at the Mn-cluster, *Phys. Chem. Chem. Phys. 6*, 4733−4736.
12. Kamiya, N., and Shen, J.-R. (2003) Crystal structure of oxygen-evolving photosystem II from *Thermosynechococcus vulcanus* at 3.7 Å resolution, *Proc. Natl. Acad. Sci. U.S.A. 100*, 98−103.
13. Loll, B., Kern, J., Saenger, W., Zouni, A., and Biesiadka, J. (2005) Towards complete cofactor arrangement in the 3.0 Å resolution structure of photosystem II, *Nature 438*, 1040−1044.
14. Koulougliotis, D., Innes, J. B., and Brudvig, G. W. (1994) Location of chlorophyll$_Z$ in photosystem II, *Biochemistry 33*, 11814−11822.
15. Stewart, D. H., Cua, A., Chisholm, D. A., Diner, B. A., Bocian, D. F., and Brudvig, G. W. (1998) Identification of histidine 118 in the D1 polypeptide of photosystem II as the axial ligand to chlorophyll Z, *Biochemistry 37*, 10040−10046.
16. Wang, J., Gosztola, D., Ruffle, S. V., Hemann, C., Seibert, M., Wasielewski, M. R., Hille, R., Gustafson, T. L., and Sayre, R. T. (2002) Functional asymmetry of photosystem II D1 and D2 peripheral chlorophyll mutants of *Chlamydomonas reinhardtii*, *Proc. Natl. Acad. Sci. U.S.A. 99*, 4091−4096.
17. Tracewell, C. A., Cua, A., Stewart, D. H., Bocian, D. F., and Brudvig, G. W. (2001) Characterization of carotenoid and chlorophyll photooxidation in photosystem II, *Biochemistry 40*, 193−203.
18. Schenck, C. C., Diner, B., Mathis, P., and Satoh, K. (1982) Flash-induced carotenoid radical cation formation in photosystem II, *Biochim. Biophys. Acta 680*, 216−27.
19. De Las Rivas, J., Telfer, A., and Barber, J. (1993) Two coupled β-carotene molecules protect P680 from photodamage in isolated Photosystem II reaction centers, *Biochim. Biophys. Acta 1142*, 155−164.
20. Telfer, A., Dhami, S., Bishop, S. M., Phillips, D., and Barber, J. (1994) β-carotene quenches singlet oxygen formed by isolated photosystem II reaction centers, *Biochemistry 33*, 14469−14474.
21. Noguchi, T., Mitsuka, T., and Inoue, Y. (1994) Fourier transform infrared spectrum of the radical cation of β-carotene photoinduced in photosystem II, *FEBS Lett. 356*, 179−182.
22. Pascal, A., Telfer, A., Barber, J., and Robert, B. (1999) Fourier transform resonance Raman spectra of cation carotenoid in photosystem II reaction centres, *FEBS Lett. 453*, 11−14.
23. Hanley, J., Deligiannakis, Y., Pascal, A., Faller, P., and Rutherford, A. W. (1999) Carotenoid oxidation in photosystem II, *Biochemistry 38*, 8189−8195.
24. Vrettos, J. S., Stewart, D. H., de Paula, J. C., and Brudvig, G. W.(1999) Low-temperature optical and resonance Raman spectra of a carotenoid cation radical in photosystem II, *J. Phys. Chem. B 103*, 6403−6406.
25. Faller, P., Pascal, A., and Rutherford, A. W. (2001) β-carotene redox reactions in photosystem II: Electron-transfer pathway, *Biochemistry 40*, 6431−6440.
26. Tracewell, C. A., and Brudvig, G. W. (2003) Two redox active β-carotene molecules in photosystem II, *Biochemistry 42*, 9127−9136.
27. Lakshmi, K. V., Poluektov, O. G., Reifler, M. J., Wagner, A. M., Thurnauer, M. C., and Brudvig, G. W. (2003) Pulsed high-frequency EPR study on the location of carotenoid and chlorophyll cation radicals in photosystem II, *J. Am. Chem. Soc. 125*, 5005−5014.
28. Telfer, A., Frolov, D., Barber, J., Robert, B., and Pascal, A. (2003) Oxidation of the two β-carotene molecules in the photosystem II reaction center, *Biochemistry 42*, 1008−1015.
29. Tracewell, C. A., Cua, A., Bocian, D. F., and Brudvig, G. W. (2005) Resonance Raman spectroscopy of carotenoids in photosystem II core complexes, *Photosynth. Res. 83*, 45−52.
30. Shen, J.-R., and Kamiya, N. (2005) 3D crystal structure of the photosytem II core, in *Photosystem II:* The Light-Driven Water: Plastoquinone Oxidoreductase (Wydrzynski, T., and Satoh, K., Eds.) pp 449−467, Springer, Dordrecht, The Netherlands.
31. Visser, J. W. M., Rijgersberg, C. P., and Gast, P. (1977) Photooxidation of chlorophyll in spinach chloroplasts between 10 and 180 K, *Biochim. Biophys. Acta 460*, 36−46.

32. Thompson, L. K., and Brudvig, G. W. (1988) Cytochrome *b*-559 may function to protect photosystem II from photoinhibition, *Biochemistry 27*, 6653−6658.
33. Hillmann, B., and Schlodder, E. (1995) Electron-transfer reactions in Photosystem II core complexes from Synechococcus at low temperature−difference spectrum of $P680^+Q_A^-$/$P680Q_A$ at 77 K, *Biochim. Biophys. Acta 1231*, 76−88.
34. Vasil'ev, S., Brudvig, G. W., and Bruce, D. (2003) The X-ray structure of photosystem II reveals a novel electron transport pathway between P680, cytochrome b_{559} and the energy quenching cation, Chl_Z^+, *FEBS Lett. 543*, 159−163.
35. Ishikita, H., and Knapp, E. W. (2005) Redox potentials of chlorophylls and β-carotene in the antenna complexes of photosystem II, *J. Am. Chem. Soc. 127*, 1963−1968.
36. Buser, C. A., Thompson, L. K., Diner, B. A., and Brudvig, G. W. (1990) Electron-transfer reactions in manganese-depleted photosystem II, *Biochemistry 29*, 8977−8985.
37. Bautista, J. A., Tracewell, C. A., Schlodder, E., Cunningham, F. X., Jr., Brudvig, G. W., and Diner, B. A. (2005) Construction and characterization of genetically modified *Synechocystis* sp. PCC 6803 photosystem II core complexes containing carotenoids with shorter π-conjugation than β-carotene, *J. Biol. Chem. 280*, 38839−38850.
38. Faller, P., Maly, T., Rutherford, A. W., and MacMillan, F. (2001) Chlorophyll and carotenoid radicals in photosystem II studied by pulsed ENDOR, *Biochemistry 40*, 320−326.
39. Faller, P., Rutherford, A. W., and Un, S. (2000) High field EPR study of carotenoid$^+$ and the angular orientation of chlorophyll $z^{\bullet+}$ in photosystem II, *J. Phys. Chem. B 104*, 10960−10963.
40. Noguchi, T., and Berthomieu, C. (2005) Molecular analysis by vibrational spectroscopy, in *Photosystem II: The Light-Driven Water: Plastoquinone Oxidoreductase* (Wydrzynski, T., and Satoh, K., Eds.) pp 367−387, Springer, Dordrecht, The Netherlands.
41. Noguchi, T., and Inoue, Y. (1995) Molecular interactions of the redox active accessory chlorophyll on the electron donor side of photosystem II as studied by Fourier transform infrared spectroscopy, *FEBS Lett. 370*, 241−244.
42. Ono, T., and Inoue, Y. (1986) Effects of removal and reconstitution of the extrinsic 33, 24 and 16 kDa proteins on flash oxygen yield in photosystem II particles, *Biochim. Biophys. Acta 850*, 380−389.
43. Berthomieu, C., Nabedryk, E., Mäntele, W., and Breton, J. (1990) Characterization by FTIR spectroscopy of the photoreduction of the primary quinone acceptor Q_A in photosystem II, *FEBS Lett. 269*, 363−367.
44. Noguchi, T., Tomo, T., and Inoue, Y. (1998) Fourier transform infrared study of the cation radical of P680 in the photosystem II reaction center: Evidence for charge delocalization on the chlorophyll dimer, *Biochemistry 37*, 13614−13625.
45. Onoda, K., Mino, H., Inoue, Y., and Noguchi, T. (2000) An FTIR study on the structure of the oxygen-evolving Mn-cluster of photosystem II in different spin forms of the S_2 state, *Photosynth. Res. 63*, 47−57.
46. Ashikawa, I., Kito, M., Satoh, K., Koike, H., Inoue, Y., Saiki, K., Tsukida, K., and Koyama, Y. (1987) All-trans β-carotene-5,6-epoxide in thylakoid membranes, *Photochem. Photobiol. 46*, 269−75.
47. Gao, Y., and Kispert, L. D. (2003) Reaction of carotenoids and ferric chloride: Equilibria, isomerization, and products, *J. Phys. Chem. B 107*, 5333−5338.
48. Fiedor, J., Fiedor, L., Haessner, R., and Scheer, H. (2005) Cyclic endoperoxides of β-carotene, potential pro-oxidants, as products of chemical quenching of singlet oxygen, *Biochim. Biophys. Acta 1709*, 1−4.
49. Nabedryk, E., Leonhard, M., Mäntele, W., and Breton, J. (1990) Fourier transform infrared difference spectroscopy shows no evidence for an enolization of chlorophyll a upon cation formation either in vitro or during P700 photooxidation, *Biochemistry 29*, 3242−3247.

BI052346Y